Cell Reports, Volume *28*

Supplemental Information

Conformational Sensors and Domain Swapping Reveal Structural and Functional Differences between β-Arrestin Isoforms

Eshan Ghosh, Hemlata Dwivedi, Mithu Baidya, Ashish Srivastava, Punita Kumari, Tomek Stepniewski, Hee Ryung Kim, Mi-Hye Lee, Jaana van Gastel, Madhu Chaturvedi, Debarati Roy, Shubhi Pandey, Jagannath Maharana, Ramon Guixà-González, Louis M. Luttrell, Ka Young Chung, Somnath Dutta, Jana Selent, and Arun K. Shukla

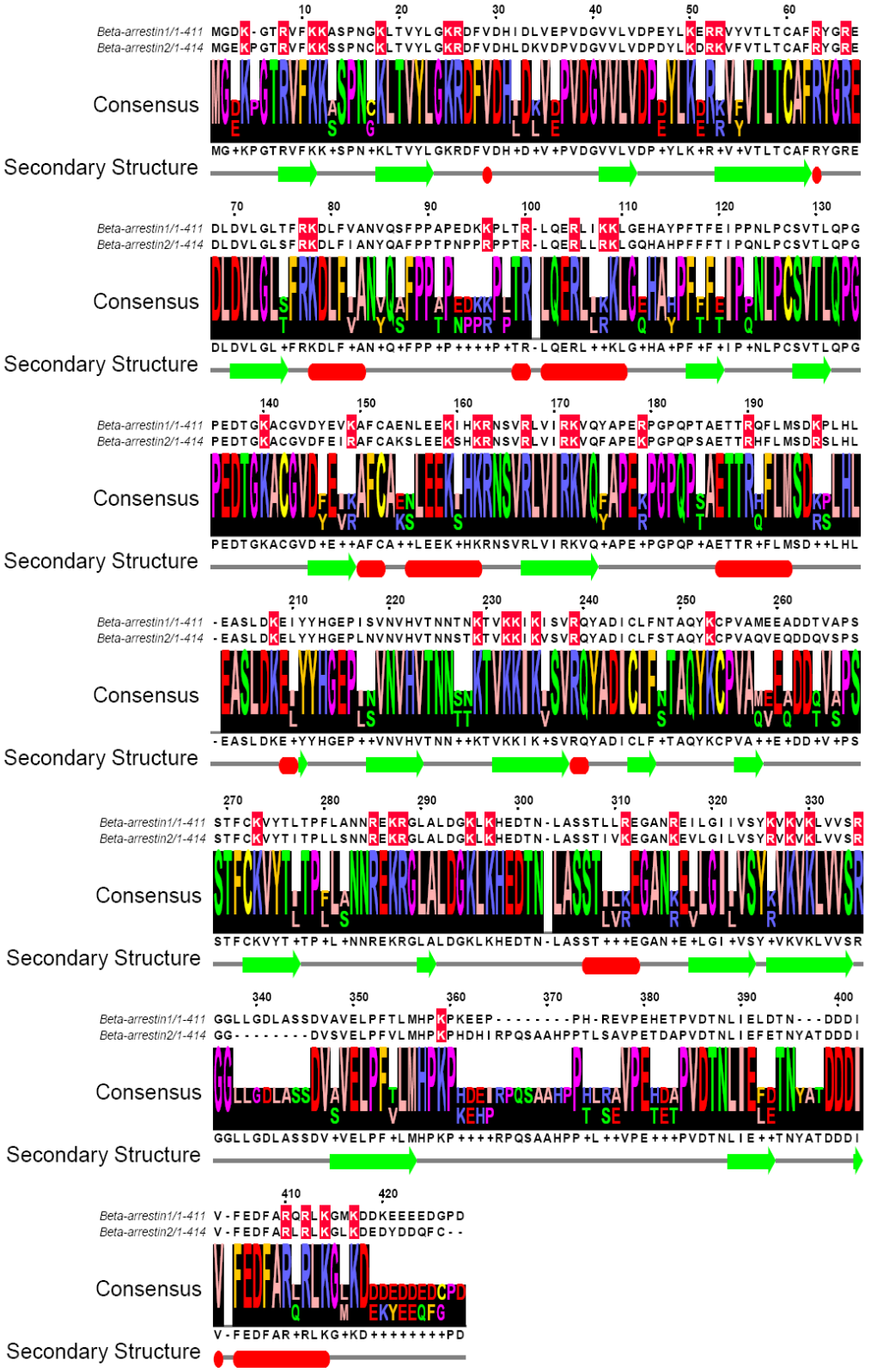

Supplemental Figure S1. Overall sequence conservation between βarr1 and 2. Related to Figure 1. Sequences of bovine βarr1 and 2 were aligned using the default T-Coffee and the alignment reliability was evaluated by Core/TCS tool. The aligned sequence was visualized and analyzed in Jalview program. Conserved Lys and Arg are highlighted in red. Shown below the alignment are Consensus Annotation and Sequence Logo. Secondary structure bar depicts JNetPRED annotation (The consensus prediction - helices are marked as red tubes, and sheets as dark green arrows) done by JNet secondary structure prediction in Jalview.

A.

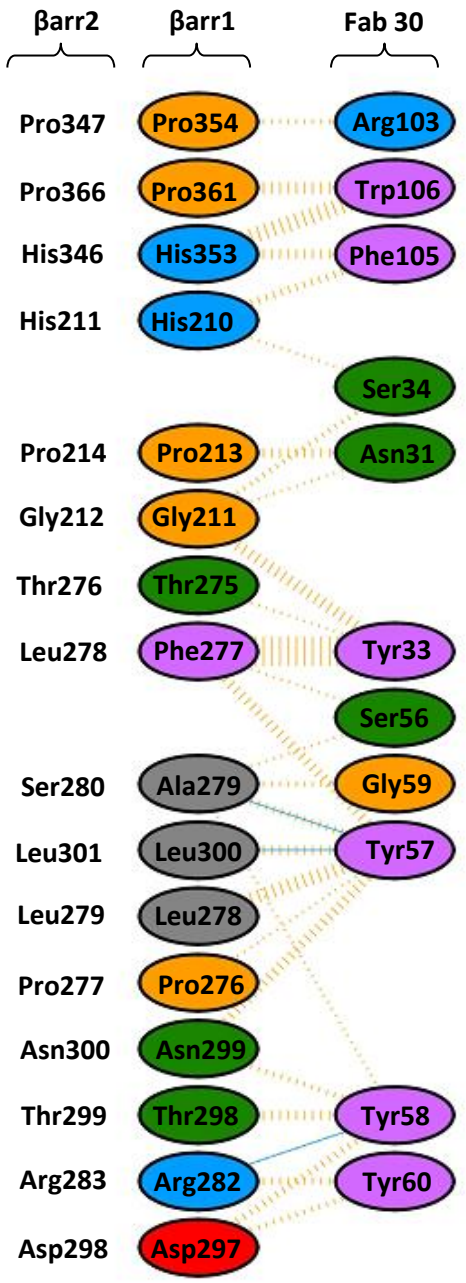

B.

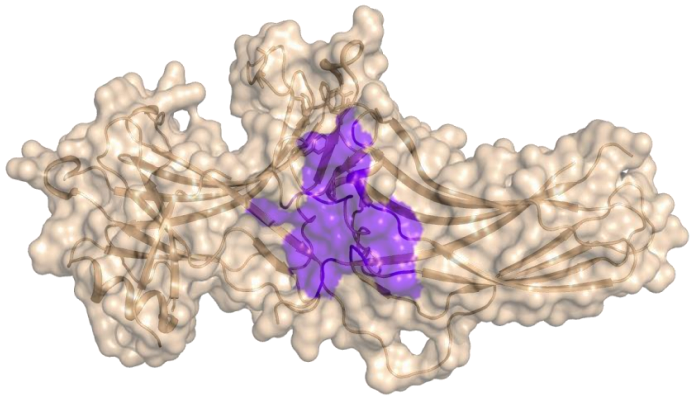

C.

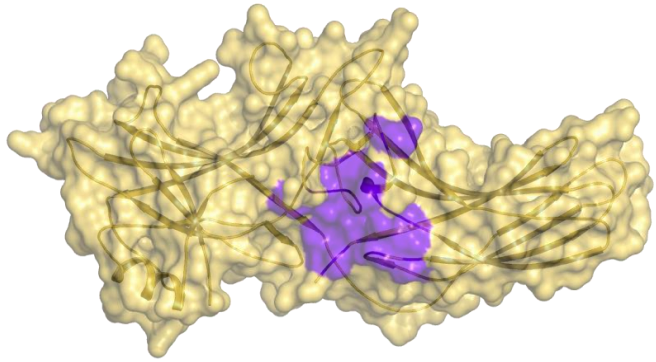

Supplemental Figure S2. Fab30 interacting residues on βarr1 and 2 are well conserved. Related to Figure 2. A. Schematic representation of amino acid residues in βarr1 that interact with Fab30 based on previously determined crystal structure (PDB ID: 4JQI). Coordinates of the crystal structure were submitted into *PDBSum*, and the interactions were mapped as a simplified ladder. **B.** The epitope of Fab30 on βarr1 is mapped on the crystal structure of V_2Rpp-bound βarr1. **C.** Amino acid residues in βarr1 that form the epitope of Fab30 are also conserved in βarr2 as mapped on the crystal structure (PDB ID: 3P2D).

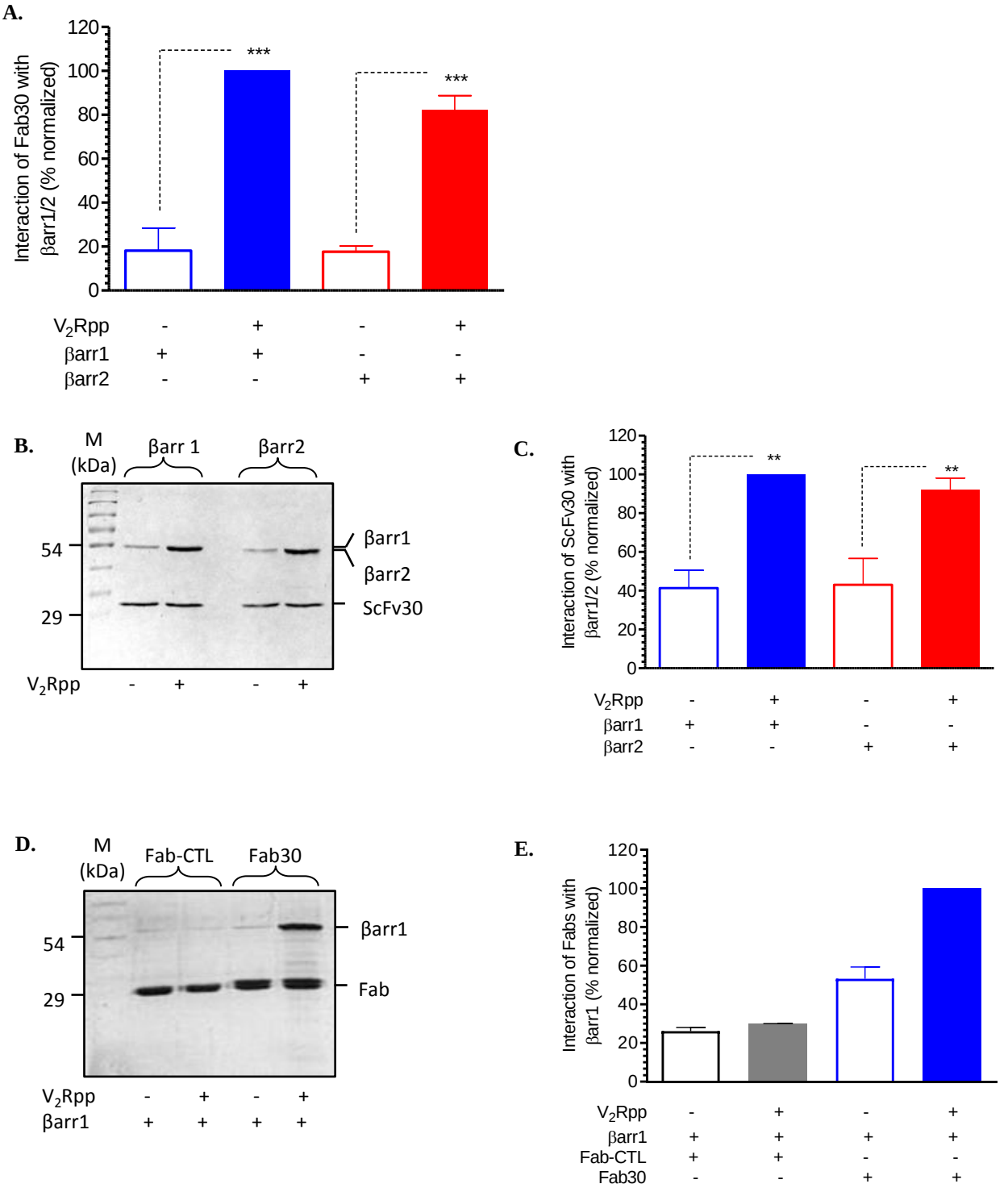

Supplemental Figure S3. Reactivity of Fab30 and ScFv30 towards V_2Rpp-bound βarr1/2. Related to Figure 1. A. Densitometry-based quantification of data presented in Figure 1E. Mean±SEM of three independent experiments are presented. **B.** Purified ScFv30 was incubated with V_2Rpp-bound βarr1 or 2 followed by co-immunoprecipitation using protein L beads. The interaction between ScFv30 and βarrs was visualized using Western blotting. **C.** Densitometry-based quantification of data presented in panel B. Mean±SEM of three independent experiments are presented and data are normalized with respect to maximum signal for V_2Rpp-βarr1 condition (treated as 100%). Data were analyzed using One-Way ANOVA with Bonferroni post-test (***$p<0.001$; **$p<0.01$). **D-E.** A control Fab, referred to as Fab-CTL, that does not interact with βarrs, exhibits no significant reactivity towards V_2Rpp-bound βarr1 as assessed by co-IP assay. These experiments are carried out under the same experimental condition as in Figure 1D-E.

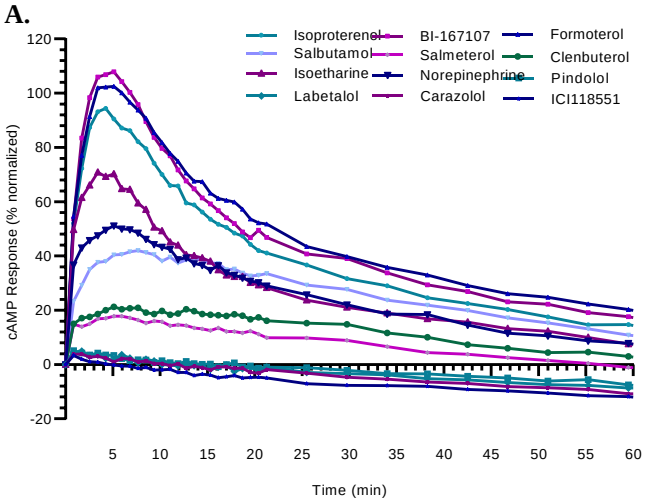

B.

Ligand	Integrated cAMP response
Isoproterenol	100.0 ± 0.0
BI-167107	122.6 ± 6.9
Formoterol	126.5 ± 8.6
Salbutamol	66.8 ± 9.0
Salmeterol	21.3 ± 5.1
Clenbuterol	29.8 ± 6.5
Pindolol	2.4 ± 1.4
Isoetharine	70.1 ± 9.1
Norepinephrine	63.8 ± 9.4
Labetalol	2.4 ± 1.5
Cara	2.0 ± 1.3
ICI118551	1.0 ± 0.8

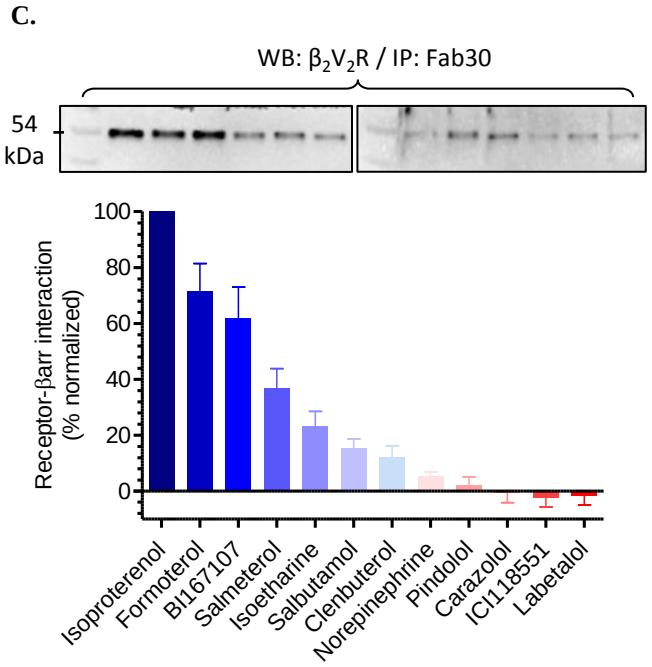

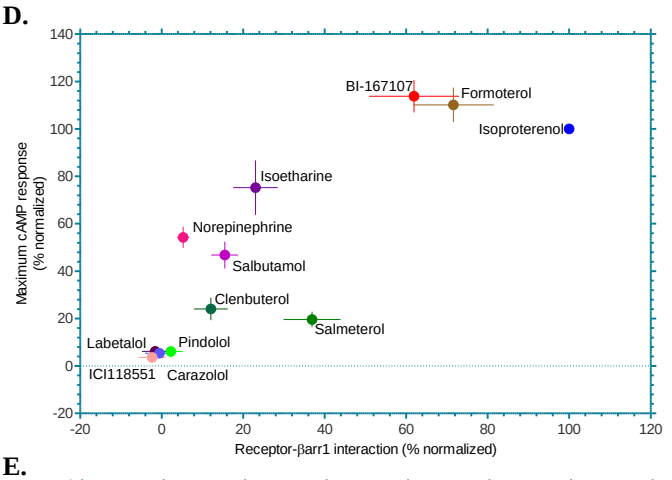

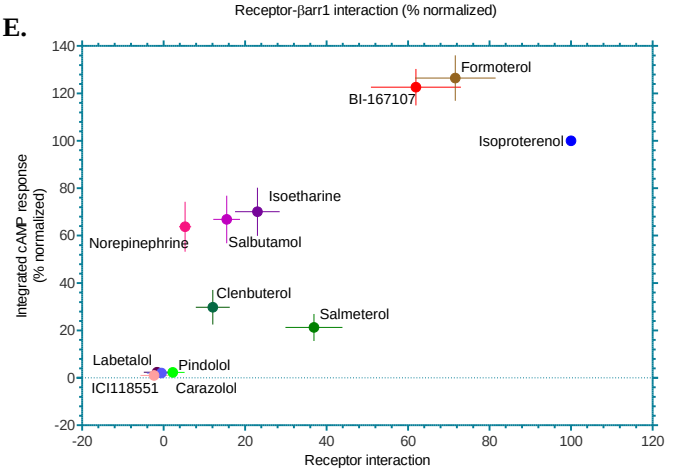

Supplementary Figure S4. Correlation between ligand efficacy and Fab30 reactivity towards receptor-bound βarr1. Related to Figure 2. A. cAMP response of twelve different β_2AR ligands using the Glo-sensor assay. HEK-293 cells expressing endogenous β_2AR were transfected with F-22 plasmid and stimulated with the saturating dose of ligands. Subsequently, the levels of cAMP were recorded for an extended time-period and plotted in GraphPad Prism. Data represent average of 5 independent experiments and normalized with isoproterenol response (treated as 100%). **B.** Quantitation of the integrated cAMP response (calculated as area under the curve) based on the data presented in panel A. The values in the right column indicated normalized response (mean±SEM) with respect to isoproterenol. **C.** Reactivity of Fab30 with receptor-bound βarr1. *Sf*9 cells expressing β_2V_2R were stimulated with saturating concentration of indicated ligands (1=Isoproterenol, 2=BI167107, 3=Formoterol,4=Salbutamol, 5=Salmeterol, 6=Clenbuterol, 7=Pindolol, 8=Isoetharine, 9=Norepinephrine, 10=Labetalol, 11=Carazolol, 12=ICI118551). Subsequently, cells were lysed, incubated with purified βarr1 and Fab30 followed by co-immunoprecipitation using protein L beads. Samples were subsequently visualized by Western blotting using HRP-coupled anti-FLAG M2 antibody. A representative image from six independent experiments is presented here and the densitometry-based quantification of all six experiments is presented in the lower panel. **D-E.** Correlation between cAMP response (maximum values or integrated response based on data presented in panel A-B) and the reactivity of Fab30 towards receptor-bound βarr1 as presented in panel C.

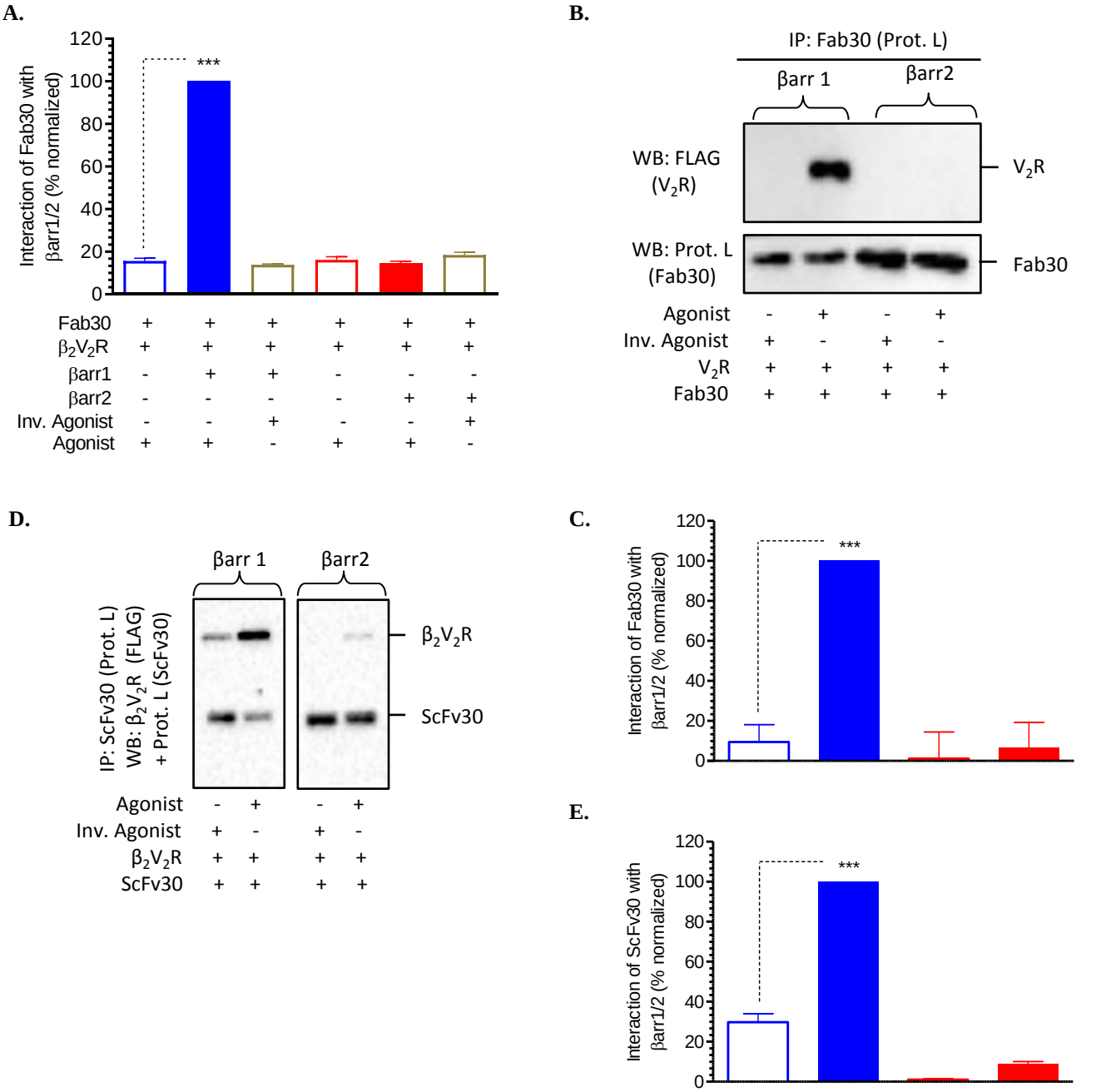

Supplemental Figure S5. Reactivity of Fab30/ScFv30 towards receptor-bound βarr1 and 2. Related to Figure 2. A. The reactivity of Fab30 towards β_2V_2R-bound βarr1 and 2 were measured in an ELISA assay. First, purified Fab30 was immobilized in polystyrene plates, followed by the addition of β_2V_2R and either βarr1 or 2. Afterwards, the wells were washed extensively and the captured β_2V_2R was visualized using HRP-coupled anti-FLAG M2 antibody. Data represent mean±SEM of three independent experiments, each carried out in duplicate. Data are normalized with respect to maximum signal for agonist+β_2V_2R+βarr1_Fab30 condition (treated as 100%) and analyzed using One-Way ANOVA with Bonferroni post-test (***$p<0.001$). **B-C.** Co-immunoprecipitation assay reveals selective recognition of V_2R-bound βarr1 but not βarr2 by Fab30. This coIP experiment was performed in a similar fashion as described in Figure 2A. Panel C shows densitometry based quantification of data, and values represent mean±SEM of three independent experiments analyzed using One-Way ANOVA with Bonferroni post-test (***$p<0.001$). Data are normalized with respect to agonist-V_2R-βarr1-Fab30 condition (treated as 100%). Here, Tolvaptan (1μM) is used as an inverse agonist while AVP (1μM) is used as an agonist to stimulate the cells expressing FLAG-tagged V_2R. **D-E.** Co-immunoprecipitation assay reveals selective recognition of receptor-bound βarr1 but not of βarr2 by ScFv30. This coIP experiment was performed in a similar fashion as described for Fab30 in Figure 2A. Panel E shows densitometry based quantification of data, and values represent mean±SEM of three independent experiments analyzed using One-Way ANOVA with Bonferroni post-test (***$p<0.001$). Data are normalized with respect to agonist-β_2V_2R-βarr1-ScFv30 condition (treated as 100%).

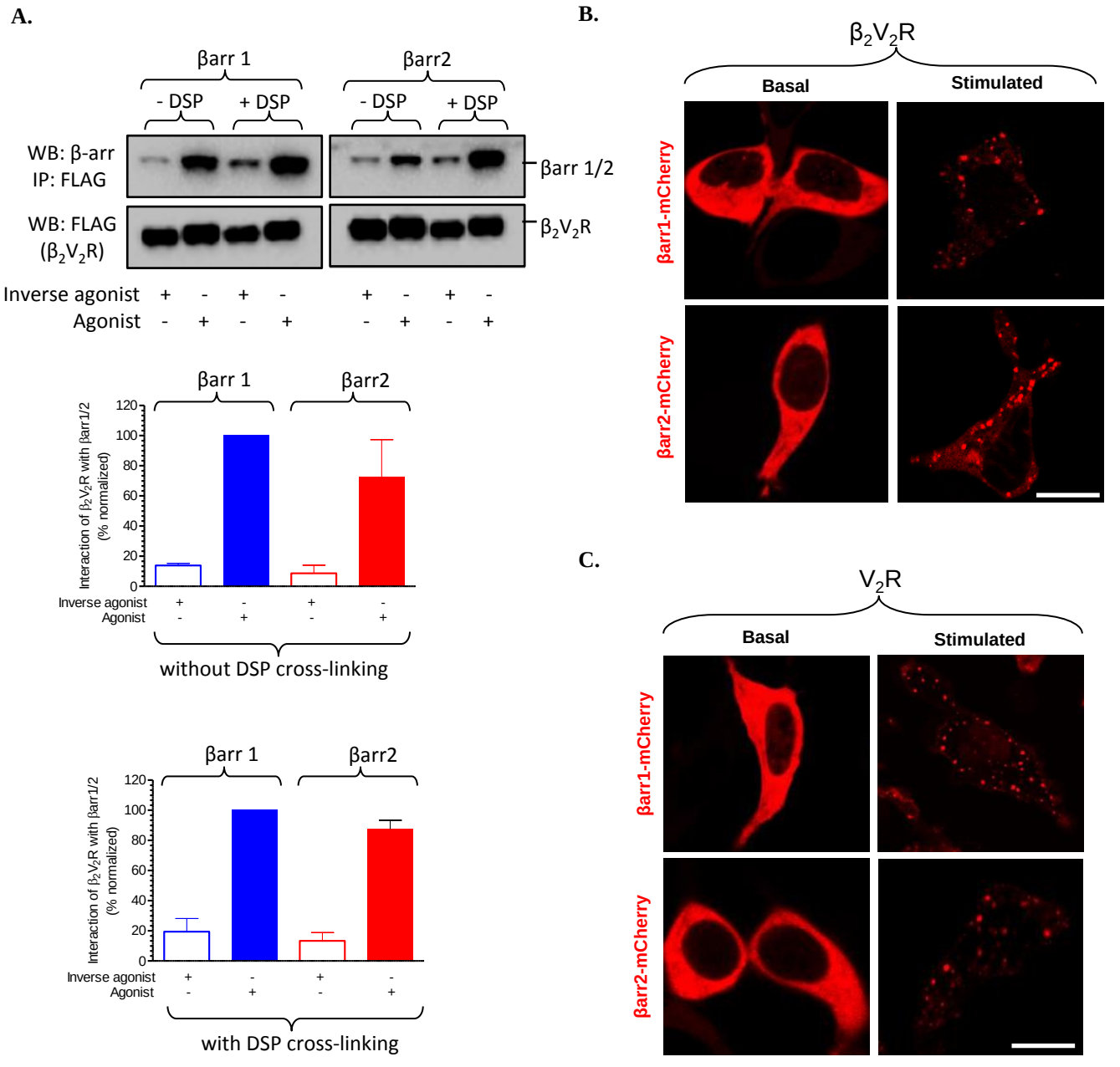

Supplemental Figure S6. β_2V_2R and V_2R recruit βarr2 upon agonist-stimulation. Related to Figure 2. A. *Sf*9 cells expressing β_2V_2R were stimulated with either an inverse agonist (carazolol) or full agonist (BI-167107). Subsequently, cells were lysed and equal amounts of purified βarr 1 or 2 were added. β_2V_2R was immunoprecipitated using anti-FLAG M1 antibody agarose and the interaction of βarr 1 and 2 was visualized by Western blotting. In another set, a cross-linking reaction was also performed with 1mM DSP (dithiobis succinimidyl propionate) after mixing the cell lysate with βarrs followed by co-immunoprecipitation experiment. We observed comparable interaction of both βarr1 and 2 with β_2V_2R. These experiments were carried out twice with identical results and a representative image is shown. The lower panels show densitometry based quantification of β_2V_2R-βarr interaction, and data are normalized with respect to agonist-β_2V_2R-βarr1 condition (treated as 100%). **B.** β_2V_2R recruits βarr1/2 upon agonist-stimulation as visualized by confocal microscopy. HEK-293 cells expressing β_2V_2R and βarr1/2-mCherry were stimulated with 10μM isoproterenol. Subsequently, the recruitment and internalization of β_2V_2R-bound βarr1/2 in endosomal vesicles was visualized by confocal microscopy. **C.** V_2R recruits βarr1/2 upon agonist-stimulation as visualized by confocal microscopy. HEK-293 cells expressing V_2R and βarr-mCherry were stimulated with AVP (100nM). Subsequently, the recruitment and internalization of V_2R-bound βarr2 in endosomal vesicles was visualized by confocal microscopy. The images presented in the right panels are captured after 20min of agonist stimulation and scale bar is 10μm.

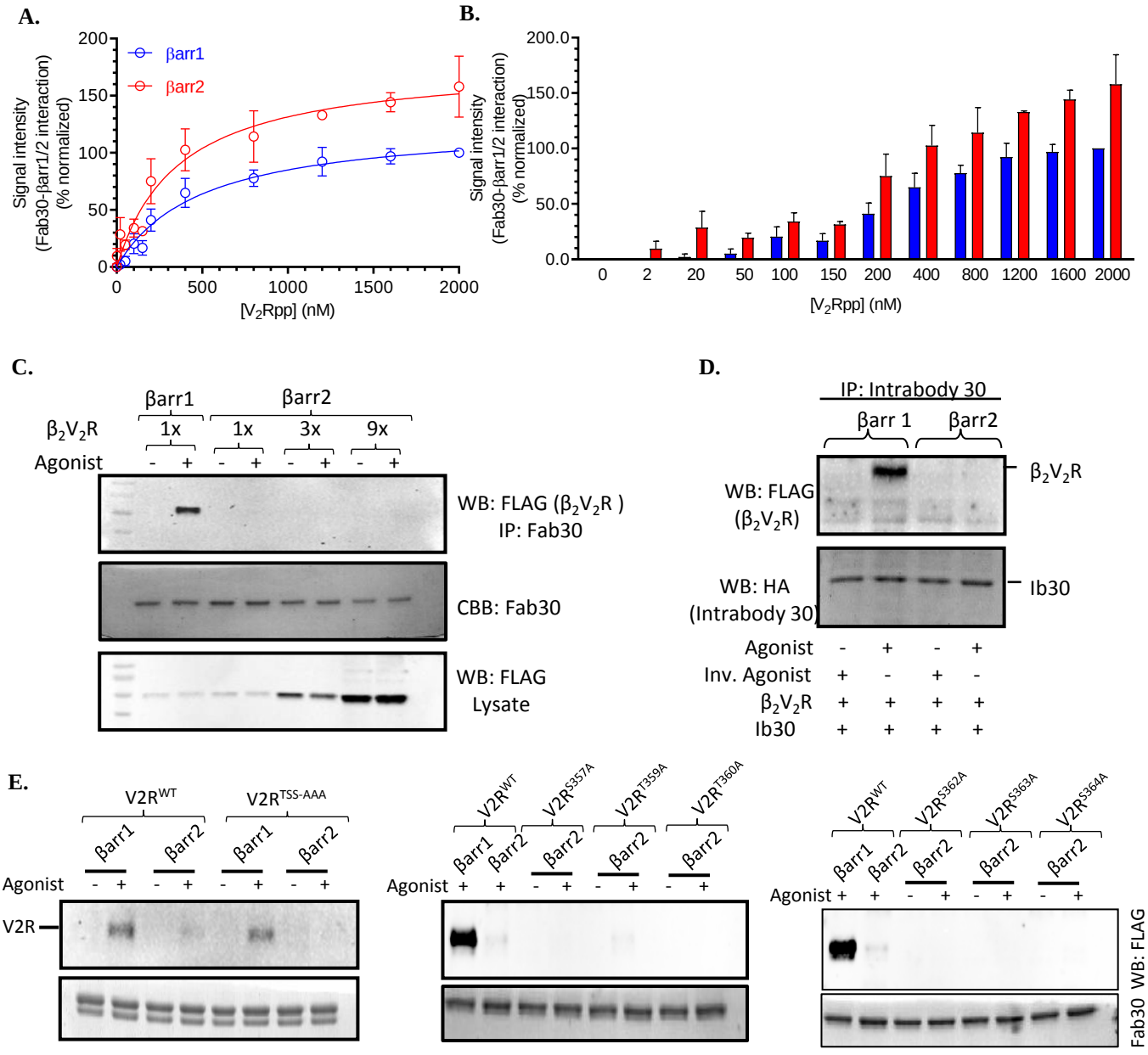

Supplemental Figure S7. Receptor titration, intrabody30 co-IP and phospho-site mutants corroborate the potential structural differences between βarr1 and 2. Related to Figure 2. (A-B) Purified βarr1/2 (200nM) were incubated with increasing concentrations of V_2Rpp (as indicated in the figure) followed by ELISA experiment to measure the reactivity by Fab30. We observed that Fab30 recognizes V_2Rpp-bound βarr2 as efficiently as βarr1, even at partial occupancy with V_2Rpp. Data represent mean±SEM of three independent experiments, each carried out in duplicate. **(C)** Purified βarr1/2 were incubated with Fab30 and cellular lysate prepared from *Sf*9 cells expressing β_2V_2R. Despite using up-to nine-fold more β_2V_2R, we still did not observe any detectable reactivity of Fab30 towards receptor-bound βarr2. This finding indicates that the lack of Fab30 reactivity is not due to stoichiometric differences in terms of available phosphorylated carboxyl-terminus. **(D)** Intrabody 30 (Ib30) confirms distinct conformations of receptor-bound βarr1 and 2 in cellular context. HEK-293 cells were transfected with β_2V_2R, βarr1/2 mcherry and Ib30 followed by co-immunoprecipitation experiment using the HA tag on Ib30. The interaction of Ib30 with receptor-βarr complexes was visualized by Western blotting. A representative image from two independent experiments is presented here. **(E)** A series of V_2R mutants were generated harboring site-specific mutations of distinct phosphorylation sites in the carboxyl-terminus. HEK-293 cells expressing either WT or mutant V_2R constructs were stimulated with agonist (AVP; 100nM, 30 min), lysed, incubated with purified βarr1/2 and Fab30. Subsequently, co-IP experiment was performed using protein L agarose beads and proteins were detected using Western blot. Similar to WT receptor, Fab30 did not exhibit any detectable recognition of receptor-bound βarr2 for any of the receptor mutants. A representative image of two independent experiments are shown here.

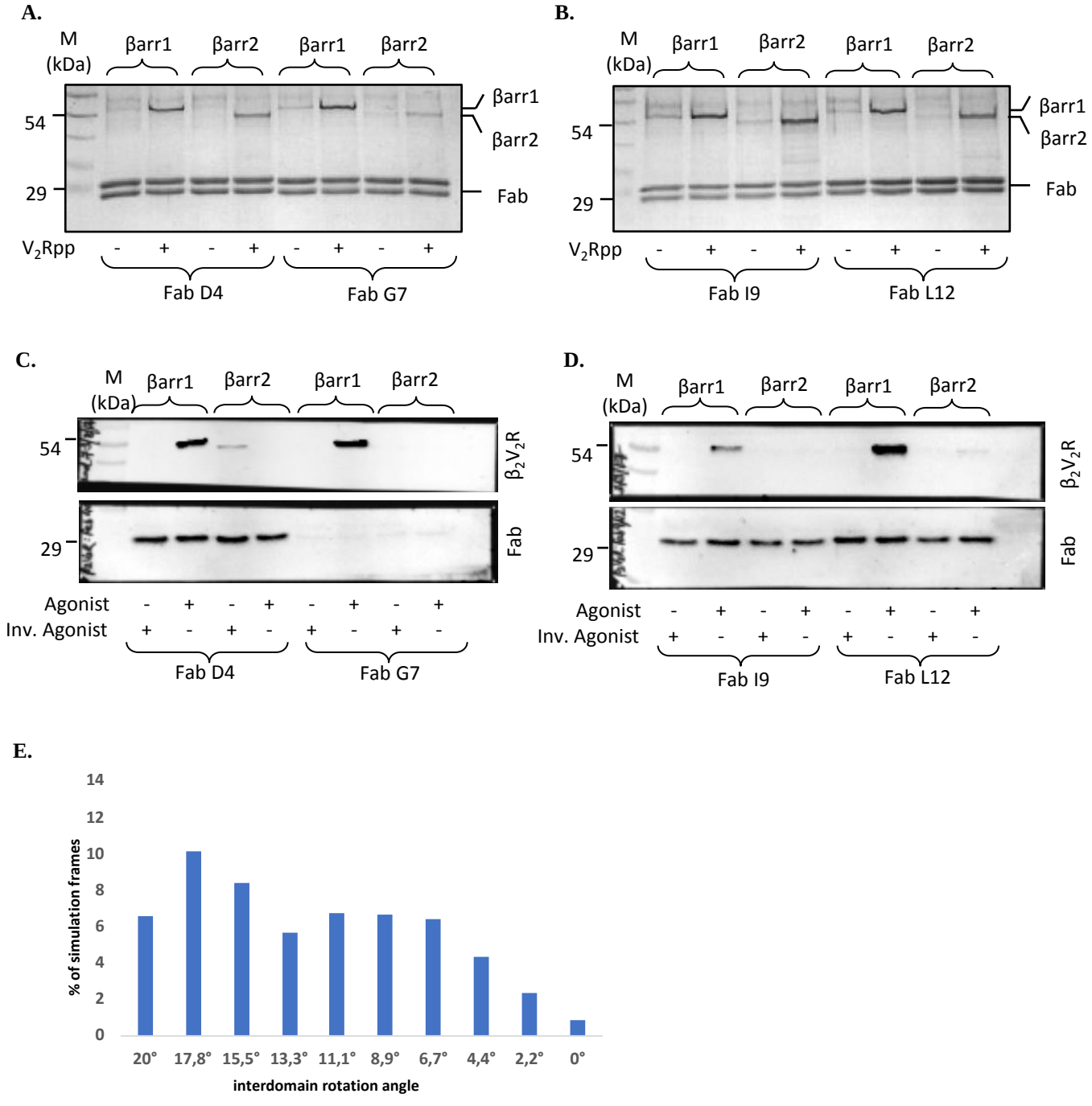

Supplemental Figure S8. Additional Fab sensors and MD simulation corroborate the structural differences between βarr1 and 2. Related to Figure 2-3. (A-B) A set of additional Fabs reveal conformational similarity between V_2Rpp-bound βarr1 and 2. Purified βarr1 or 2 were incubated with the indicated Fab in absence or presence of V_2Rpp followed by co-immunoprecipitation using Protein L beads and visualization using SimplyBlue (SB) staining. A representative image of two independent experiments is shown. **(C-D)** Reactivity pattern of these additional Fabs supports conformational differences between β_2V_2R-bound βarr1 and 2. *Sf*9 cells expressing FLAG-β_2V_2R were stimulated with either an agonist (BI167107, 1µM) or inverse agonist (Carazolol, 1µM) for 1h followed by incubation with purified βarr1 or 2 and indicated Fabs. Afterwards, the receptor was solubilized using 1% MNG and co-immunoprecipitated using Protein L beads. Samples were visualized by Western blotting using HRP-coupled anti-FLAG M2 antibody (for β_2V_2R) and HRP-coupled Protein L (for Fabs). For some reason, FabG7 is not stained well with HRP-coupled Protein L but Ponceau staining of the membrane shows equal amount of Fab pull-down. **(E)** The presence of interpolated states along the inactivation pathway (unbiased simulation) is quantified as percentage of frames with an RMSD of backbone atoms of β-sheets < 1 Å (related to Figure 3C-D).

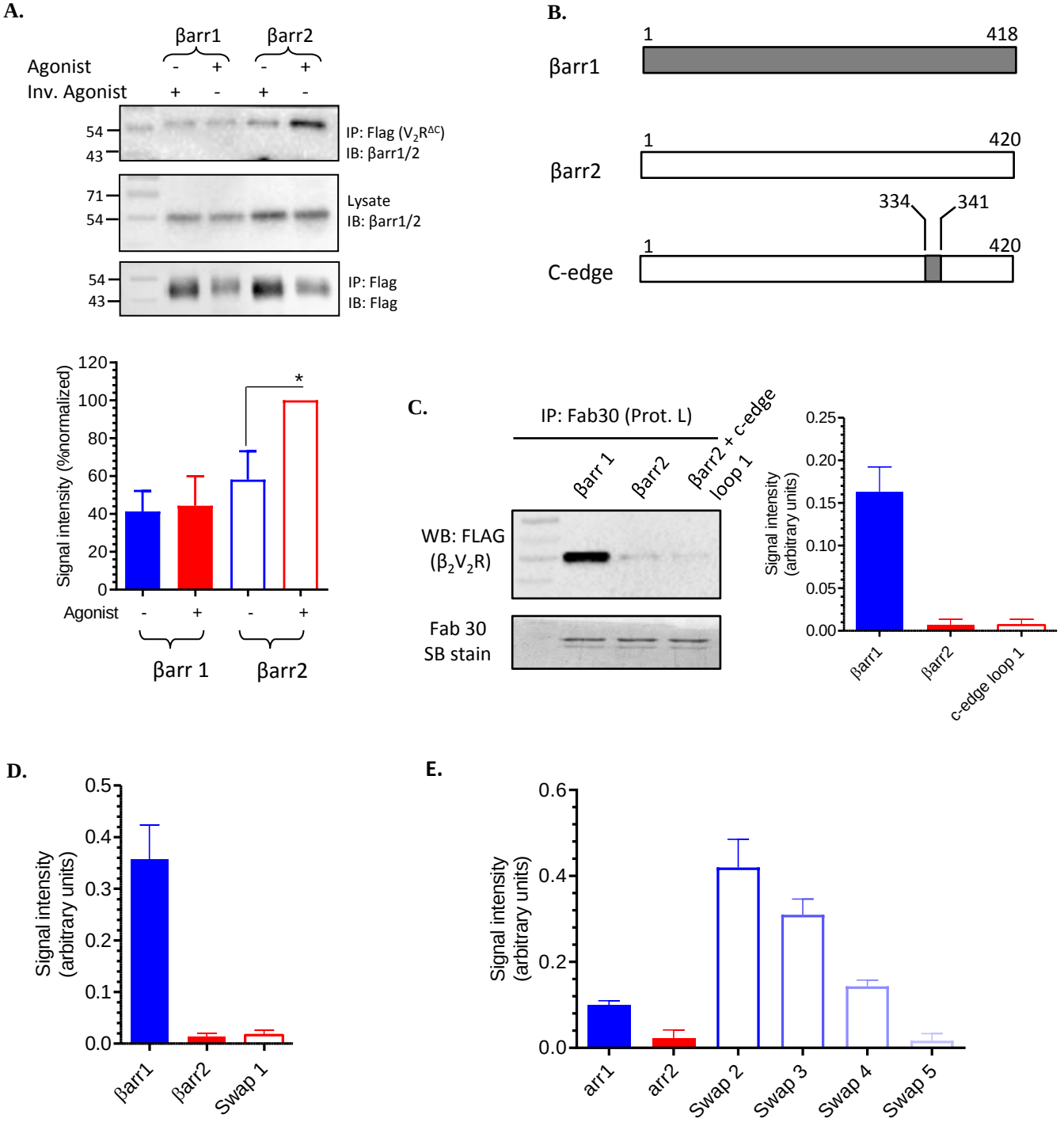

Supplemental Figure S9. Reactivity of Fab30 with chimeric βarr constructs. Related to Figures 4-5.. **(A)** HEK-293 cells were transfected with carboxyl-terminus truncated V_2R i.e. Flag-$V_2R^{\Delta C\text{-term}}$ and βarr1/2 followed by stimulation with indicated ligands, cross-linking and co-IP using anti-Flag antibody agarose. Proteins were visualized on Western blots using corresponding antibodies. A representative image of three independent experiments is shown. The lower panel shows densitometry-based quantification of data is presented after normalization with respect to agonist+βarr2 condition treated as 100%. **(B)** Schematic representation of βarr2 construct with grafted C-edge loop 1 from βarr1. **(C)** Co-IP experiment reveals that Fab30 fails to detect receptor-bound conformation of βarr2 construct with grafted C-edge loop 1. This co-IP experiment was performed following the same protocol as described in Figure 2A. A representative image of three independent experiment is presented here, and densitometry based quantification of three independent experiments is presented in the right panel. **(D)** Densitometry based quantification of data presented in Figure 4B showing the Fab30 reactivity patterns towards βarr1, 2 and swap1. **(E)** Densitometry based quantification of data presented in Figure 4D showing the Fab30 reactivity patterns towards βarr1, 2 and swap2-5.

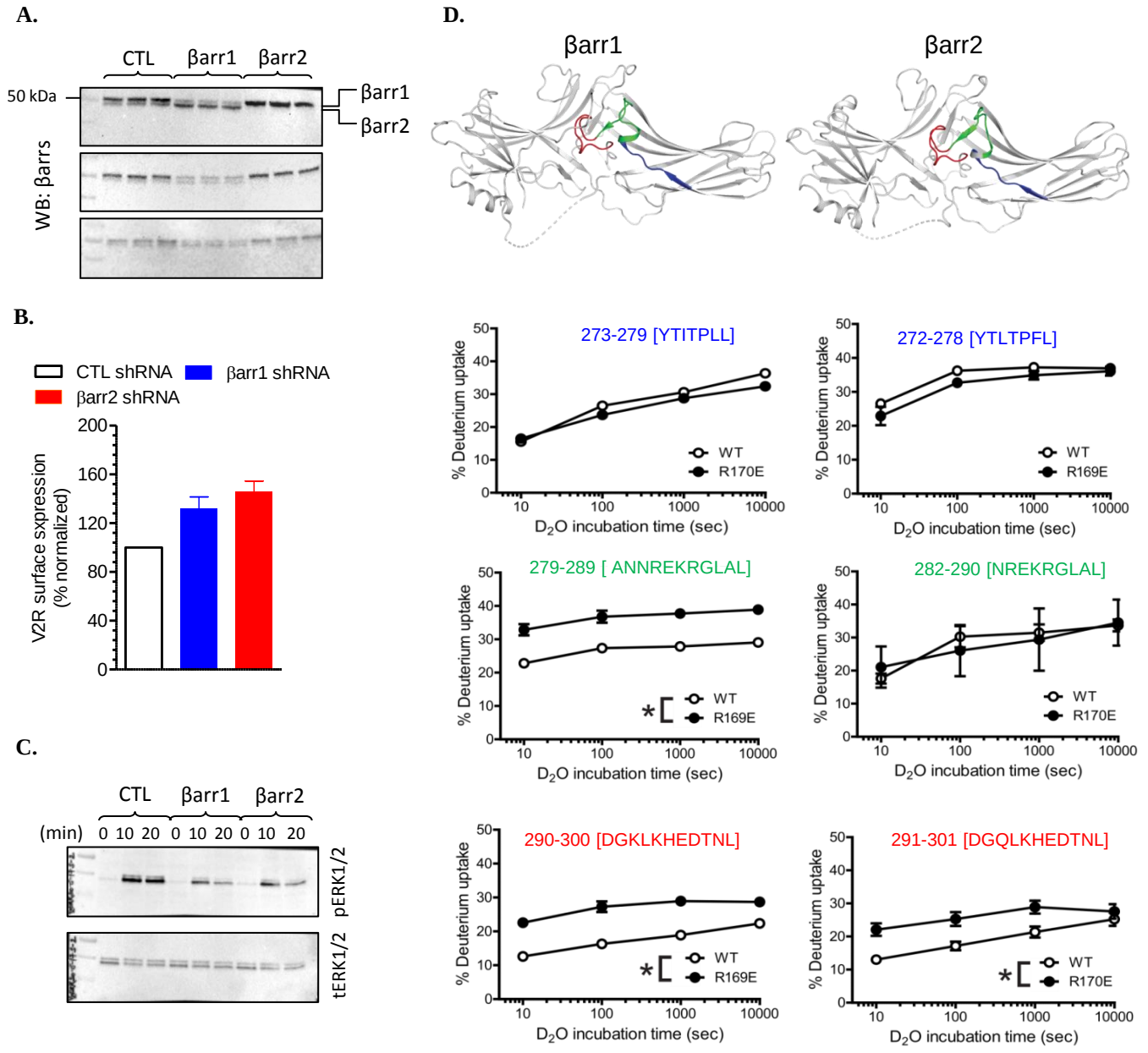

Supplemental Figure S10. βarr knock-down and Hydrogen/Deuterium exchange analysis to probe functional and structural differences of βarr isoforms. Related to Figure 5. (A) Western blot analysis of lysates prepared from HEK-293 cells stably expressing CTL-shRNA, βarr1-shRNA and βarr2-shRNA to measure βarr knock-down levels**.** Lysates from three different wells of a six-well plate are shown from three different experiments. **(B)** Surface expression of V_2R was comparable in cells transfected with CTL, βarr1 and βarr2 shRNA as measured by whole cell ELISA assay. Data are normalized with respect to V_2R expression in CTL shRNA transfected cells (treated as 100%). **(C)** Agonist-induced ERK activation downstream of V_2R depends on both βarr1 and 2 as revealed by comparing the ERK phosphorylation in cells transfected with CTL, βarr1 and βarr2 shRNA. These experiments were carried out five times with identical results and a representative image is shown. Densitometry based quantification of data from all five experiments presented in Figure 5D. **(D)** Hydrogen-deuterium exchange analysis of wild-type βarr1/2 and their pre-activated, polar core mutants ($\beta arr1^{R169E}\beta arr2^{R170E}$) reveal significant differences in deuterium uptake between the two isoforms suggesting a conformational difference. We specifically highlight the HDX pattern observed in the lariat loop region color coded in the structural snapshot in the top panels. The original HDX data on βarrs and their pre-activated mutants have been published earlier (Yun et al., 2015), and the deuterium uptake for the peptides in the lariat loop region are re-analyzed here. The uptake plots are represented as mean±SEM of three independent experiments and analyzed using T-test (*$p<0.05$).